Synthesis of C60/[10]CPPCatenanes by Regioselective, NanocapsuleTemplated Bingel BisAddition

How to cite: *Angew. Chem. Int. Ed.* **2023**, *62*, e202309393
doi.org/10.1002/anie.202309393

Catenanes

Synthesis of C_{60}/[10]CPP-Catenanes by Regioselective, Nanocapsule-Templated Bingel Bis-Addition

Fabian M. Steudel, Ernest Ubasart, Luigi Leanza, Míriam Pujals, Teodor Parella, Giovanni M. Pavan, Xavi Ribas,* and Max von Delius**

Abstract: The addition of two unsymmetric malonate esters to the Buckminster fullerene C_{60} can lead to 22 spectroscopically distinguishable isomeric products and therefore represents a formidable synthesis challenge. In this work, we achieve 87 % selectivity for the formation of a single (*in*,*out*-*trans*-3) isomer by combining three approaches: (i) we use a starting material, in which the two malonates are covalently connected (tether approach); (ii) we form the strong supramolecular complex of C_{60} with the shape-persistent [10]CPP macrocycle (template approach) and (iii) we embed this complex further within a self-assembled nanocapsule (shadow mask approach). Variation of the spacer chain shed light on the limitations of the approach and the ring dynamics in the unusual [2]catenanes were studied in silico with atomistic resolution. This work significantly widens the scope of mechanically interlocked architectures comprising cycloparaphenylenes (CPP).

[*] F. M. Steudel, Prof. M. von Delius
Institute of Organic Chemistry, Ulm University
Albert-Einstein-Allee 11, 89081 Ulm (Germany)
E-mail: max.vondelius@uni-ulm.de

Dr. E. Ubasart, M. Pujals, Prof. X. Ribas
Institut de Química Computacional i Catàlisi, Universitat de Girona
C/M. Aurèlia Capmany 69, 17003 Girona, Catalonia (Spain)
E-mail: xavi.ribas@udg.edu

L. Leanza, Prof. G. M. Pavan
Department of Applied Science and Technology, Politecnico di Torino
Corso Duca degli Abruzzi, 24, 10129 Torino (Italy)
E-mail: giovanni.pavan@polito.it

Dr. T. Parella
Servei de Ressonància Magnètica Nuclear, Universitat Autònoma de Barcelona
Campus UAB, Bellaterra, 08193 Barcelona, Catalonia (Spain)

Prof. G. M. Pavan
Department of Innovative Technologies, University of Applied Sciences and Arts of Southern Switzerland, Polo Universitario Lugano, Campus Est
Via la Santa 1, 6962 Lugano-Viganello (Switzerland)

Introduction

Inspired by observations on the superior performance of isomerically pure fullerene bis-adducts in third-generation solar cells,[1] the chemo-, itero,-[2] regio- and stereoselective[3] multiple functionalization of fullerenes has witnessed a renaissance in the past ten years.[4] The classic approach to the regioselectivity problem of bis-addition has been pioneered by Diederich[5] and relies on the use of bifunctional tethers. Hirsch and Nierengarten have developed cleavable tethers,[6] which are particularly attractive for further functionalization of the installed addends. Supramolecular approaches that do not rely on the formation of macrocyclic products have also been developed over the past seven years.[7] These include the use of the [10]CPP macrocycle,[7d] which by itself offers imperfect selectivity for two regioisomers (*trans*-2 and *trans*-3), and the use of a supramolecular Pd-based nanocapsule[7a,8] as shadow mask, which furnished exclusive *e* selectivity (i.e. functionalization along the equatorial belt of C_{60}).[7e] By joining these two approaches, we recently reported a three-shell matryoshka-like complex that facilitated exclusive *trans*-3 selectivity (Figure 1, top).[7f]

The regioselectivity problem of C_{60} bis-addition becomes significantly more challenging, if unsymmetric functional groups are added to the fullerene double bonds. A total number of 22 spectroscopically distinguishable regioisomers and diastereomers can be formed in that case (36 isomers

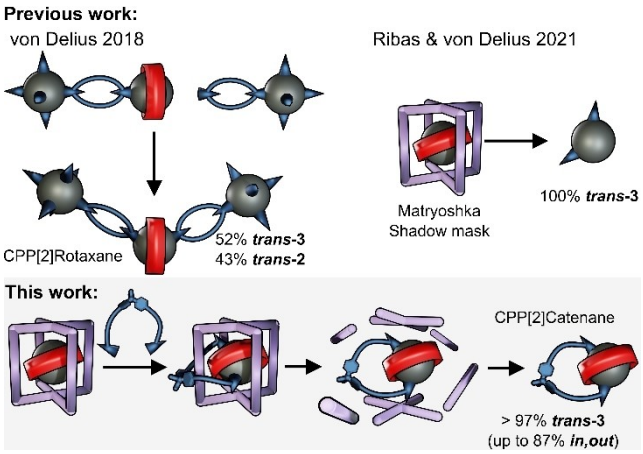

Figure 1. Concept behind the present work and relevant prior work (percentage values correspond to observed isomeric ratios). [10]CPP ring shown in red.

including enantiomers),[9] as compared to only eight in the case of symmetric addends.[10] In this work, we answer the question whether our matryoshka-like approach is suitable to deliver selective reaction outcomes even when unsymmetric reagents are used. We found that selectivity for the *trans*-3 double bond is still excellent, and that one of the three *trans*-3 diastereomers, which only differ in the relative orientation of the unsymmetric addends, can be obtained with a remarkable relative yield of up to 87 %. Because our reaction products have [2]catenane topology, this work represents a new addition to the small set of mechanically interlocked architectures based on shape-persistent carbon nanohoops[7d,11] and fullerene bis-adducts.[12]

Results and Discussion

Our molecular design for the envisaged C_{60}/[10]CPP catenanes comprises two bromomalonate units that are connected via alkyl chains and a central bisphenol A (**BPA**) unit. The **BPA** moiety serves a dual purpose, namely to harness the Thorpe–Ingold (gem-dimethyl) effect and to act as an indicator for strain in molecular mechanics calculations of the initial macrocyclic products (Figure S1). The obtained molecular models indicated that a tetradecyl (**C14**) spacer was nearly unstrained with a phenyl to phenyl C–C bond angle of 109.7° that is nearly identical to the 109.5° found in linear reference compounds. Because the goal of this study was not only to prepare a new type of [2]catenane, but also to test and understand the limits of supramolecular, three-shell regiocontrol, we decided to carry out catenane syntheses with a set of four spacers (**C13**, **C14**, **C15** and **C16**).

As shown in Figure 2a, the bis-bromomalonates (**BBM**) were synthesized over two steps, by etherification of **BPA** with the respective bromoalcohols **1**–**4**, followed by esterification with the α-brominated acid bromide **5**. The latter was obtained via Hell-Volhard-Zelinsky reaction from methyl hydrogen malonate (**MHM**). To complete the synthesis of the desired **C13-** to **C16-Catenanes**, a 2.5-fold

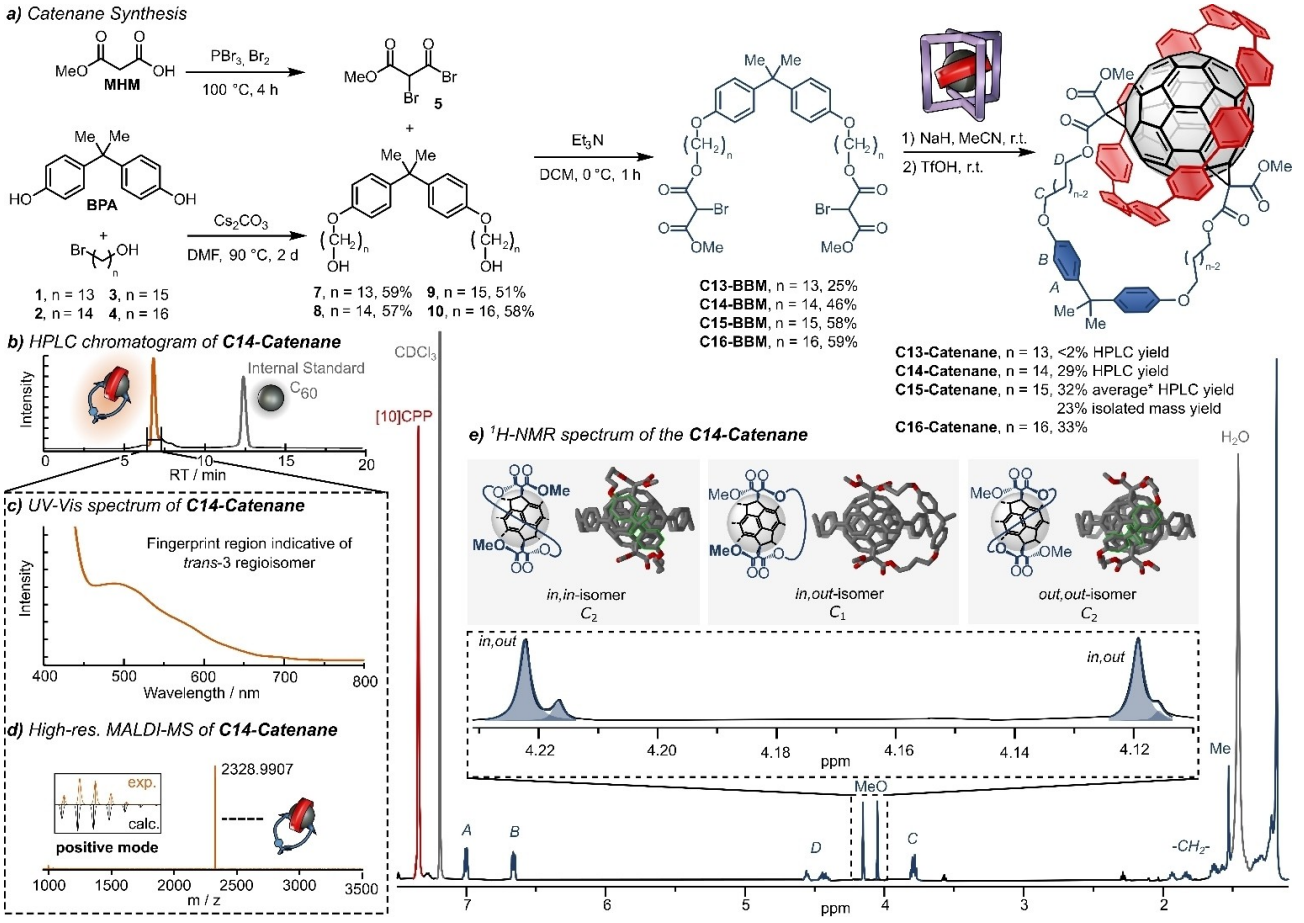

Figure 2. a) Syntheses of the **C13-** to **C16-Catenanes**. *: Average HPLC yield of three experiments. b) Representative HPLC chromatogram of **C14-Catenane** (6.3–8.1 min, Buckyprep M, toluene, 0.5 mL/min) with internal standard $\mathbf{C_{60}}$ for determination of HPLC yields. c) UV/Vis spectrum generated by photodiode array detector during HPLC, averaged for 6.6–7.1 min retention time. d) Representative high resolution matrix assisted laser desorption/ionization mass spectrometry (MALDI-MS; positive mode) of the purified **C14-Catenane** including isotopic pattern. e) ^{1}H NMR spectrum (600 MHz, $CDCl_3$, 298 K) of the **C14-Catenane** with assignment of the *in,out*-isomer signals and a zoom region (600 MHz, $CDCl_3$, 298 K) of the methyl ester (MeO) signals showing four singlets due to the formation of three different *trans*-3 isomers. Grey boxes: schematic and calculated (Ghemical) structures of the *in,in*-, *in,out*- and *out,out*-isomers.

excess of the bis-bromomalonates was added to a solution of the three-shell complex comprising nanocapsule **6**·$(BArF)_8$, [10]CPP and C_{60} (previously reported in ref. [7f]) in acetonitrile, and a Bingel bis-addition reaction[13] was carried out using an excess of sodium hydride as base. The formation of the catenanes in the presence of the nanocapsule was monitored by high resolution mass spectrometry (HRMS) with an electron spray ionization (ESI) ion source (Figure S10–S13). After completion of the reaction, the nanocapsule was disassembled by addition of trifluoromethanesulfonic acid (20 equiv.) and subjected to analysis by high-performance liquid chromatography (HPLC).

For the bis-bromomalonates with sufficiently long spacers (**C14**–**C16**), we obtained HPLC yields (with internal standard and calibrated for extinction coefficient) around 30 % (Figure 2b) in the crude samples. Because the crude HPLC traces (see Figure S15–S17) show no noticeable side products, we attribute these moderate yields to incomplete conversion. Purification of the crude samples by semi-preparative HPLC followed by precipitation from toluene with *n*-pentane led to some loss of material (e.g. 23 % isolated mass yield for the **C15-Catenane**), which is however not surprising at this small reaction scale.

For bis-bromomalonate **C13-BBM**, the spacer appears to be too short to allow significant conversion to the **C13-Catenane** and hence no product could be isolated. In the successful syntheses of the **C14**-, **C15**- and **C16-Catenanes**, the formation of the *trans*-3 regioisomer was confirmed by analyses of the "fingerprint region" of the UV/Vis spectrum (Figure 2c). Further confirmation of this assignment was obtained by carrying out a transesterification reaction between the **C15-Catenane** and methanol (Figure S6–8) and comparison of the ^{1}H NMR data with suitable reference compounds **S11a–d**. This experiment also revealed that a small quantity (<3 %) of the *trans*-2 isomer was formed (potentially due to background reaction outside degraded nanocapsule), which demonstrates the utility of this type of experiment.[14] The identity of the samples as monomers and [2]catenanes was confirmed by high-resolution (tandem) mass spectrometry (Figure 2d and Figure S27–28).

A diffusion coefficient of $4.9\cdot10^{-10}$ m^2s^{-1} was obtained by diffusion ordered NMR spectroscopy (DOSY, Figure S34). As expected, the calculated solvodynamic radius of ≈8.1 Å is slightly larger than that of non-catenated fullerene bisadducts.[15] The ^{1}H NMR spectra of the products (Figure 2e and Figure S30–S33) showed splitting of the methyl ester "CH_3" signals into four singlets with pairs of two peaks at chemical shifts of ca. 4.22 ppm and 4.12 ppm, respectively. This finding is expected for any Bingel bis-adducts with unsymmetric malonates (here: OMe and O-tether)[16] and is due to the splitting of the *trans*-3 regioisomer into three distinct diastereomers that differ in the relative orientations of malonate OMe substituents (see Figure 2e: *in,in*, *in,out* and *out,out*).

Having realized that the four singlets in the "OMe" region belong to three *in,out*-isomers, we turned our attention to their assignment in the ^{1}H NMR spectrum. Because the *in,out*-isomer exhibits C_1 symmetry, this isomer should show two different singlets integrating in a ratio of 1:1. When inspecting the ^{1}H NMR spectrum shown in Figure 2e with this knowledge, it is evident that the two predominant singlets, which integrate with near-perfect 1:1 ratio must belong to the *in,out*-isomer. However, since the *in,in*- and *out,out*-isomers exhibit C_2 symmetry, each of these isomers should only show a single OMe signal in the ^{1}H NMR spectrum and their chemical/magnetic environment should differ significantly, as becomes evident by comparison with the ^{1}H NMR spectra of dimethyl malonate fullerene bisadduct reference compounds (Figure S38). Each of these symmetrical isomers exhibit one single singlet but with a very similar chemical shift as its counterpart of the *in,out*-isomer. Since the tentative assignment of these OMe peaks by ROESY NMR (Figure S35) to the respective *in,in*- and *out,out*-isomers remained elusive, we denominated these as (b) and (c) (see Figure 3 and Table 1). In all the catenanes the aromatic [10]CPP signals appear as a singlet at 7.4 ppm, thus confirming the rapid [10]CPP rotation around the fullerene system on the NMR time scale.

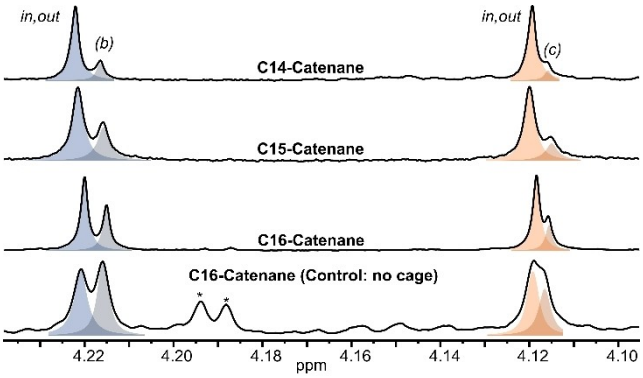

Figure 3. ^{1}H NMR spectra (600 MHz, $CDCl_3$, 298 K) of the isolated **C14-** to **C16-Catenanes** and peak integration for the *trans*-3 methyl ester signals by deconvolution. (Other isomers in the control reaction marked by *). See Table 1 for deconvoluted *trans*-3 diastereoisomer ratios.

Table 1: HPLC yields of the **C13-** to **C16-Catenanes** and relative amounts of the three *trans*-3 diastereoisomers ("isomer fraction").[a]

Catenane	HPLC Yield	*in,out*-isomer fraction	(b)-isomer fraction	(c)-isomer fraction
C13-Catenane	<2 %[b]	n.d.	n.d.	n.d.
C14-Catenane	29 %	**87 %**	8 %	5 %
C15-Catenane	32±4 %[c] (23 %)[d]	74±2 %[c]	17±1 %[c]	9±2 %[c]
C16-Catenane	33 %	70 %	19 %	11 %
C16 no cage[e]	<13 %[d,e]	54 %	27 %	19 %

[a] All HPLC yields determined using C_{60} as internal standard and calibrated for extinction coefficient. All isomer fractions determined by ^{1}H NMR spectroscopy (see Figure 3); [b] upper limit according to quantitative HPLC. N.d.: isomer fraction could not be determined due to insufficient quantity; [c] Average results of three experiments with error corresponding to standard deviation; [d] yields determined by weighing after isolation by preparative HPLC; [e] sample obtained by reaction with [10]CPP, but without nanocapsule.

Because we were unable to resolve the isomer mixtures by HPLC (e.g. Buckyprep, Buckyprep-M), we proceeded to draw quantitative conclusions on the isomer distributions that are evidently different for the **C14**, **C15** and **C16** tethers (Figure 3; spectra recorded via cryoprobe at 600 MHz). Despite the high magnetic field, partial peak overlap was observed, which is why we resorted to peak deconvolution in lieu of classic integration (software MNova) as detailed in Table 1. We found that the fraction of the *in,out-trans*-3 isomer was maximal (i.e., 87 %) for the **C14-Catenane**. Lower fractions of 70–74 % for this same isomer were observed in the **C15-** and **C16-Catenanes**, whereas a statistical isomer distribution was observed in a control experiment with the **C16-BBM** starting material (Figure 3, bottom and Table 1), where only the nanocapsule was omitted from the reaction mixture (such a statistical isomer mixture was also observed in a study by Brabec and co-workers on indane bis-adducts of C_{60}).[1a]

We conclude from the data presented in Table 1 that the *trans-3* isomer distribution that is intrinsic for this type of reaction (in the absence of any template) is close to the statistical ratio of 2:1:1 for the *in,out-*, *in,in-* and *out,out*-isomers, respectively. The presence of the [10]CPP ring alone is not sufficient for altering this statistical isomer distribution (experiment "C16 no cage" in Table 1). The combination of [10]CPP with the nanocapsule and a rather generous tether length (as in **C16**) however leads to an altered isomer ratio of ca. 70:20:10, presumably due to steric reasons largely dictated by the nanocapsule.[7f] For the shorter **C15** tether we observed a slightly higher *in,out* selectivity (isomer ratio ca. 74:17:9) and for the **C14** tether *in,out* selectivity was maximal (isomer ratio ca. 87:8:5). This finding is highly plausible, because the distance between the two malonate groups is the shortest in the *in,out-trans*-3 isomer (Figure 2e) and slightly longer in both the *in,in-* and the *out,out*-isomer. Hence, this additional tether effect must reach a lower practical limit, where the tether is too short, which indeed explains our finding that the **C13** tether largely shuts down (bis-addition) reactivity (less than 2 % total yield, see Table 1, top).

To gain insights into the dynamics of the **C14-Catenane**, we have employed all-atom molecular simulations, in particular pertaining to the [10]CPP rotation, tilting and translation around the larger ring. As recently demonstrated with rotaxanes[17a] and supramolecular polymers,[18] we combined classical molecular dynamics (MD) and infrequent well-tempered metadynamics (WT-MetaD)[19] to characterize the dynamical behavior of this C_{60}/[10]CPP catenane. The atomistic model of the **C14-Catenane** (*in,out-trans*-3 isomer) shown in Figure 4a was built and parametrized consistent with our recent work on a related rotaxane (see Methods section in the supporting information for details).[17a] The catenane model (Fig 4a) was immersed in a periodic box filled with explicit chloroform solvent molecules and, after preliminary energy minimization, equilibrated in periodic boundary (NPT) conditions at the temperature of 300 K.

As a first step, we investigated the thermodynamics and kinetics of the processes of [10]CPP unbinding from the fullerene binding site as well as [10]CPP translation around the larger ring. Figure 4b shows representative structures observed during the translation process as a function of the rotational angle around the catenane center (from 0 to 2π). Since the unbinding of [10]CPP from the fullerene requires crossing a large free-energy barrier, we used WT-MetaD simulations, recently proven very effective to study the dynamics and thermodynamics of similar architectures[17a] (see Supporting Information for computational details). This approach provided a characteristic [10]CPP escape time from the fullerene of ≈30 seconds, which agrees very well with previous literature findings[17a] and corresponds to a kinetic barrier of ≈19.3 ± 0.2 kcal/mol (see Supporting Information for details). Comparison with a related C_{60}/[10]CPP-[2]rotaxane[17a] indicates that the kinetic barrier primarily arises from the disruption of concave-convex π-π interactions and from the specific path that the [10]CPP ring needs to follow, due to the 120° angle formed between the

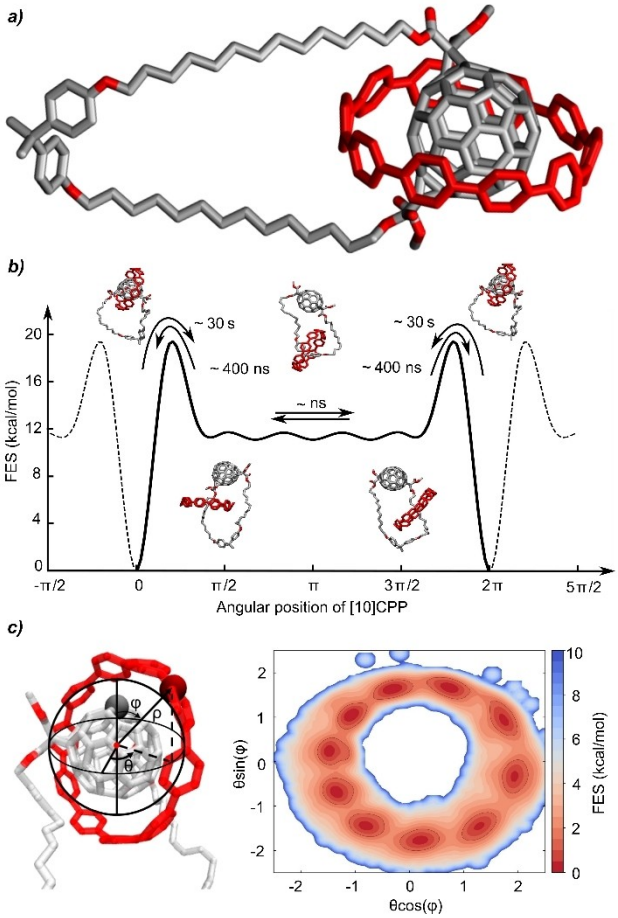

Figure 4. a) Atomistic molecular model of the **C14-Catenane** (*in,out-trans*-3 isomer). b) Free-energy diagram as a function of the angular position of [10]CPP along the larger ring of the catenane, detailing the ΔG differences and transition times between metastable states (estimated from infrequent well-tempered metadynamics). c) Left panel, schematic representation of the variables used to describe the molecular rotation of [10]CPP around the fullerene: φ is the rotation, θ is tilting and ρ is the radius. Right panel: Free-energy surface of [10]CPP angular configuration as a function of φ and θ.

malonate substituents and the fullerene core. To complete the reconstruction of the translation of [10]CPP in the catenane, we performed multiple MD simulations starting from configurations where [10]CPP is in lateral position on the aliphatic spacer chain (Figure 4b: snapshots at $\pi/2$ and $3\pi/2$) or located at the bisphenol A site (Figure 4b: snapshots at π). In all 12 replica simulations (6 starting from the lateral and 6 from the bisphenol A position), the macrocycle was seen to leave the starting configuration and diffuse along the thread re-binding with the fullerene within 1 μs of MD with an average binding time of ≈400 ns (corresponding to a kinetic barrier for binding of ≈8.5 kcal/mol). Notably, the kinetics of the [10]CPP-fullerene re-complexation was found nearly identical whether the [10]CPP starts from a lateral position on the thread or from the bisphenol group, indicating that the [10]CPP-bisphenol binding is relatively weak under these conditions and that the [10]CPP translation is controlled by the binding/unbinding with the fullerene (see Supporting Movie and free-energy translation diagram shown in Figure 4b).

As an additional step, we investigated the rotational and tilting degree of freedom of [10]CPP in the bound configuration on the fullerene. From 1 μs of MD simulation we decomposed the motion of [10]CPP in pure rotation (φ, Figure 4c, left panel) and tilting (θ).[17a] The states in Figure 4c are associated with different values of the rotation angle φ of [10]CPP around the fullerene, while the width of the distribution around the circle is associated with the tilting motion. The free-energy surface shows a circular arrangement of ten energetically equivalent minima separated by free-energy barriers of ≈2 kcal/mol. This observation indicates that under these conditions, the rotation of [10]CPP around the fullerene is a step-by-step process occurring very rapidly (≈0.1 ns to move between each minimum)[17]

Conclusion

We report syntheses of three *trans*-3 C_{60}/[10]CPP-based [2]catenanes by bis-addition of tether-based bis-bromomalonates to C_{60} encapsulated within a previously described three-shell architecture.[7f] Contrary to previous reports by our groups,[7d] the bis-bromomalonates used in this study are unsymmetric, which results in the existence of three distinct isomers that correspond to the attack of the second malonate to the same (*trans*-3) double bond on the fullerene scaffold. It is therefore remarkable that thanks to the joint action of tether, nanohoop and nanocapsule a >97% selectivity for *trans*-3 isomers and an isomer fraction of 87% for one diastereomer out of the possible three was observed. Future work by our groups will focus on fullerenes other than C_{60} and the catalytic use of the supramolecular mask, which will be necessary to produce larger quantities of products.

Experimental Section

HPLC yields. The bis-functionalization reactions were performed at very small scale (0.3–1.1 μmol; ca. 0.71–2.6 mg), because the focus of this study is primarily on selectivity and because the Pd nanocapsule is a precious material. The yields of the catenanes were therefore mainly determined by quantitative HPLC, since weighing samples of ca. 1 mg comes with significant error. Our approach for HPLC yields was such that a precise quantity of the internal standard C_{60} was added to the sample before HPLC analysis was carried out. The amount of catenane was determined from the ratio between the integrals of the catenane and the internal standard, while taking into account the difference in extinction coefficients between C_{60} and the catenanes (the catenane has higher molar extinction, since the [10]CPP also absorbs at 330 nm). Calibration for extinction coefficients was achieved with C_{60} and **C15-catenane** samples of known concentration (determined by quantitative NMR with internal standard). For one representative example (**C15-Catenane**), we also showed that isolation by preparative HPLC followed by precipitation from toluene with *n*-pentane is possible, albeit with some loss of material (see Table S2).

Acknowledgements

M.v.D. acknowledges financial support by the Deutsche Forschungsgemeinschaft (DFG) Projektnummer 182 849 149-SFB953 "Synthetic Carbon Allotropes" (project A7). X.R. thanks financial support from MINECO-Spain (PID2019-104498GB–I00, TED2021-130573B–I00), Fundación Areces (Regiosolar project) and Generalitat de Catalunya (2021SGR00475). X.R. is also grateful for ICREA-Acadèmia awards. E.U. thanks Universitat de Girona for a PhD grant. We also thank Dr. Harald Maid from the University of Erlangen-Nürnberg for NMR measurements of the **C16-Catenane**, and Serveis Tècnics de Recerca at UdG for technical support. G. M. P. acknowledges the funding received by the ERC under the European Union's Horizon 2020 research and innovation program (grant agreement no. 818776—DYNAPOL) and the computational resources provided by the Swiss National Supercomputing Center (CSCS), by CINECA and by HPC@POLITO (https://www.hpc.polito.it). Open Access funding enabled and organized by Projekt DEAL.

Conflict of Interest

The authors declare no conflict of interest.

Data Availability Statement

Details on the computational procedures for the parametrization of the molecular models and on the simulations' setup are provided in the Methods section in the ESI. Complete data and materials pertaining to the molecular simulations conducted in this study (input files, model files, raw data, analysis, etc.) are available at: https://doi.org/10.5281/zenodo.8319349. Other data that supports the findings of this study are available in the supplementary material of this article.

Keywords: Cages · Catenanes · Fullerenes · Regioselectivity · Supramolecular Dynamics

[1] a) T. Cao, N. Chen, G. Liu, Y. Wan, J. D. Perea, Y. Xia, Z. Wang, B. Song, N. Li, X. Li, Y. Zhou, C. J. Brabec, Y. Li, *J. Mater. Chem. A* **2017**, *5*, 10206–10219; b) F. Zhang, W. Shi, J. Luo, N. Pellet, C. Yi, X. Li, X. Zhao, T. J. S. Dennis, X. Li, S. Wang, Y. Xiao, S. M. Zakeeruddin, D. Bi, M. Grätzel, *Adv. Mater.* **2017**, *29*, 1606806; c) T. Umeyama, H. Imahori, *Acc. Chem. Res.* **2019**, *52*, 2046–2055; d) X. Meng, G. Zhao, Q. Xu, Z. Tan, Z. Zhang, L. Jiang, C. Shu, C. Wang, Y. Li, *Adv. Funct. Mater.* **2014**, *24*, 158–163; e) W. W. H. Wong, J. Subbiah, J. M. White, H. Seyler, B. Zhang, J. David, A. B. Holmes, *Chem. Mater.* **2014**, *26*, 1686–1689; f) W. Shi, Q. Zhuang, R. Zhou, X. Hou, X. Zhao, J. Kong, M. J. Fuchter, *Adv. Energy Mater.* **2023**, *13*, 2300054.

[2] a) R. Lavendomme, A. Leroy, M. Luhmer, I. Jabin, *J. Org. Chem.* **2014**, *79*, 6563–6570; b) R. Lavendomme, S. Zahim, G. De Leener, A. Inthasot, A. Mattiuzzi, M. Luhmer, O. Reinaud, I. Jabin, *Asian J. Org. Chem.* **2015**, *4*, 710–722; c) R. Lavendomme, I. Jabin, *Cell Rep. Phys. Sci.* **2022**, *3*, 101121.

[3] Z. Lu, T. Ronson, A. Heard, S. Feldmann, N. Vanthuyne, A. Martinez, J. Nitschke, *Nat. Chem.* **2023**, *15*, 405–412.

[4] a) S. B. Beil, M. von Delius, *Org. Mater.* **2021**, *3*, 146–154; b) L. Jia, M. Chen, S. Yang, *Mater. Chem. Front.* **2020**, *4*, 2256–2282; c) L. Đorđević, L. Casimiro, N. Demitri, M. Baroncini, S. Silvi, F. Arcudi, A. Credi, M. Prato, *Angew. Chem. Int. Ed.* **2021**, *60*, 313–320.

[5] a) C. Boudon, J. Gisselbrecht, M. Gross, L. Isaacs, H. L. Anderson, R. Faust, F. Diederich, *Helv. Chim. Acta* **1995**, *78*, 1334–1344; b) L. Isaacs, R. F. Haldimann, F. Diederich, *Angew. Chem. Int. Ed.* **1994**, *33*, 2339–2342; c) L. Isaacs, F. Diederich, R. F. Haldimann, *Helv. Chim. Acta* **1997**, *80*, 317–342; d) F. Cardullo, P. Seiler, L. Isaacs, J. F. Nierengarten, R. F. Haldimann, F. Diederich, T. Mordasini-Denti, W. Thiel, C. Boudon, J. P. Gisselbrecht, M. Gross, *Helv. Chim. Acta* **1997**, *80*, 343–371.

[6] a) F. Beuerle, N. Chronakis, A. Hirsch, *Chem. Commun.* **2005**, 3676–3678; b) F. Beuerle, A. Hirsch, *Chem. Eur. J.* **2009**, *15*, 7434–7446; c) S. Guerra, F. Schillinger, D. Sigwalt, M. Holler, J. F. Nierengarten, *Chem. Commun.* **2013**, *49*, 4752–4754; d) D. Sigwalt, F. Schillinger, S. Guerra, M. Holler, M. Berville, J. F. Nierengarten, *Tetrahedron Lett.* **2013**, *54*, 4241–4244; e) E. Meichsner, F. Schillinger, T. M. N. Trinh, S. Guerra, U. Hahn, I. Nierengarten, M. Holler, J. F. Nierengarten, *Eur. J. Org. Chem.* **2021**, 3787–3797; f) T. M. N. Trinh, F. Schillinger, S. Guerra, E. Meichsner, I. Nierengarten, U. Hahn, M. Holler, J. F. Nierengarten, *Eur. J. Org. Chem.* **2021**, 3770–3786; g) F. Schillinger, U. Hahn, S. Guerra, T. M. N. Trinh, D. Sigwalt, M. Holler, I. Nierengarten, J. F. Nierengarten, *Helv. Chim. Acta* **2023**, *106*, e202300026.

[7] a) C. Fuertes-Espinosa, M. Pujals, X. Ribas, *Chem* **2020**, *6*, 3219–3262; b) B. Chen, J. J. Holstein, A. Platzek, L. Schneider, K. Wu, G. H. Clever, *Chem. Sci.* **2022**, *13*, 1829–1834; c) G. Bottari, O. Trukhina, A. Kahnt, M. Frunzi, Y. Murata, A. Rodríguez-Fortea, J. M. Poblet, D. M. Guldi, T. Torres, *Angew. Chem. Int. Ed.* **2016**, *55*, 11020–11025; d) Y. Xu, R. Kaur, B. Wang, M. B. Minameyer, S. Gsänger, B. Meyer, T. Drewello, D. M. Guldi, M. von Delius, *J. Am. Chem. Soc.* **2018**, *140*, 13413–13420; e) C. Fuertes-Espinosa, C. García-Simón, M. Pujals, M. Garcia-Borràs, L. Gómez, T. Parella, J. Juanhuix, I. Imaz, D. Maspoch, M. Costas, X. Ribas, *Chem* **2020**, *6*, 169–186; f) E. Ubasart, O. Borodin, C. Fuertes-Espinosa, Y. Xu, C. García-Simón, L. Gómez, J. Juanhuix, F. Gándara, I. Imaz, D. Maspoch, M. von Delius, X. Ribas, *Nat. Chem.* **2021**, *13*, 420–427; g) V. Leonhardt, S. Fimmel, A. M. Krause, F. Beuerle, *Chem. Sci.* **2020**, *11*, 8409–8415; h) W. Brenner, T. K. Ronson, J. R. Nitschke, *J. Am. Chem. Soc.* **2017**, *139*, 75–78; i) B. Chen, J. J. Holstein, S. Horiuchi, W. G. Hiller, G. H. Clever, *J. Am. Chem. Soc.* **2019**, *141*, 8907–8913; j) A. Dhamija, A. Gunnam, X. Yu, H. Lee, I.-C. Hwang, Y. Ho Ko, K. Kim, *Angew. Chem. Int. Ed.* **2022**, *61*, e202209326.

[8] a) C. Fuertes-Espinosa, J. Murillo, M. E. Soto, M. R. Ceron, R. Morales-Martínez, A. Rodríguez-Fortea, J. M. Poblet, L. Echegoyen, X. Ribas, *Nanoscale* **2019**, *11*, 23035–23041; b) C. Garciá-Simón, C. Colomban, Y. A. Çetin, A. Gimeno, M. Pujals, E. Ubasart, C. Fuertes-Espinosa, K. Asad, N. Chronakis, M. Costas, J. Jiménez-Barbero, F. Feixas, X. Ribas, *J. Am. Chem. Soc.* **2020**, *142*, 16051–16063; c) C. Colomban, V. Martin-Diaconescu, T. Parella, S. Goeb, C. García-Simón, J. Lloret-Fillol, M. Costas, X. Ribas, *Inorg. Chem.* **2018**, *57*, 3529–3539.

[9] T. Liu, I. Abrahams, T. J. S. Dennis, *J. Phys. Chem. A* **2018**, *122*, 4138–4152.

[10] F. Djojo, A. Herzog, I. Lamparth, F. Hampel, A. Hirsch, *Chem. Eur. J.* **1996**, *2*, 1537–1547.

[11] a) J. May, J. Van Raden, R. Maust, L. Zakharov, R. Jasti, *Nat. Chem.* **2023**, *15*, 170–176; b) Y. Segawa, M. Kuwayama, K. Itami, *Org. Lett.* **2020**, *22*, 1067–1070; c) Y. Y. Fan, D. Chen, Z. A. Huang, J. Zhu, C. H. Tung, L. Z. Wu, H. Cong, *Nat. Commun.* **2018**, *9*, 3037; d) P. Bäuerle, M. Ammann, M. Wilde, G. Götz, E. Mena-Osteritz, A. Rang, C. A. Schalley, *Angew. Chem. Int. Ed.* **2007**, *46*, 363–368; e) J. M. Van Raden, B. M. White, L. N. Zakharov, R. Jasti, *Angew. Chem. Int. Ed.* **2019**, *58*, 7341–7345; f) C. E. Otteson, C. M. Levinn, J. M. Van Raden, M. D. Pluth, R. Jasti, *Org. Lett.* **2021**, *23*, 4608–4612; g) J. M. Van Raden, N. N. Jarenwattananon, L. N. Zakharov, R. Jasti, *Chem. Eur. J.* **2020**, *26*, 10205–10209; h) A. Bu, Y. Zhao, H. Xiao, C.-H. Tung, L.-Z. Wu, H. Cong, *Angew. Chem. Int. Ed.* **2022**, *61*, e202209449; i) H. Ishibashi, M. Rondelli, H. Shudo, T. Maekawa, H. Ito, K. Mizukami, N. Kimizuka, A. Yagi, K. Itami, *Angew. Chem. Int. Ed.* **2023**, e202310613; *Angew. Chem.* **2023**, e202310613.

[12] a) P. R. Ashton, F. Diederich, M. Gomez-lopez, J. A. Preece, M. Raymo, J. F. Stoddart, *Angew. Chem. Int. Ed.* **1997**, *36*, 1448–1451; b) Y. Nakamura, S. Minami, K. Iizuka, J. Nishimura, *Angew. Chem. Int. Ed.* **2003**, *42*, 3158–3162.

[13] C. Bingel, *Chem. Ber.* **1993**, *126*, 1957–1959.

[14] J.-F. Nierengarten, V. Gramlich, D.-C. F. Cardullo, F. Diederich, *Angew. Chem. Int. Ed.* **1996**, *35*, 2101–2103.

[15] M. Pujals, T. Pèlachs, C. Fuertes-Espinosa, T. Parella, M. Garcia-Borràs, X. Ribas, *Cell Rep. Phys. Sci.* **2022**, *3*, 100992.

[16] a) M. Taki, S. Sugita, Y. Nakamura, E. Kasashima, E. Yashima, Y. Okamoto, J. Nishimura, *J. Am. Chem. Soc.* **1997**, *119*, 926–932; b) E. Vlassiadi, PhD Thesis, Friedrich-Alexander-Universität Erlangen-Nürnberg, **2017**.

[17] a) L. Leanza, C. Perego, L. Pesce, M. Salvalaglio, M. von Delius, G. M. Pavan, *Chem. Sci.* **2023**, *14*, 6716–6729; b) M. J. Abraham, T. Murtola, R. Schulz, S. Páll, J. C. Smith, B. Hess, E. Lindahl, *SoftwareX* **2015**, *1–2*, 19–25; c) The PLUMED consortium, *Nat. Methods* **2019**, *16*, 670–673; d) G. A. Tribello, M. Bonomi, D. Branduardi, C. Camilloni, G. Bussi, *Comput. Phys. Commun.* **2014**, *185*, 604–613.

[18] D. Bochicchio, M. Salvalaglio, G. M. Pavan, *Nat. Commun.* **2017**, *8*, 147.

[19] P. Tiwary, M. Parrinello, *Phys. Rev. Lett.* **2013**, *111*, 230602.

Manuscript received: July 3, 2023
Accepted manuscript online: August 22, 2023
Version of record online: September 12, 2023